Influence of Molecular Weight on the Electrification of Linear Polyethylenes During Extrusion: Identification of Two Different Mechanisms for Charge Generation

Francisco Rodríguez-González,[1,2] José Pérez-González,[1] Lourdes de Vargas,[1] Edgard Moreno,[1] Germán González-Santos[3]

[1] *Laboratorio de Reología, Escuela Superior de Física y Matemáticas, Instituto Politécnico Nacional, Apdo. Postal 118-209, C. P. 07051, México, D. F., Mexico*

[2] *Posgrado en Ciencia e Ingeniería de Materiales, Instituto de Investigaciones en Materiales, Universidad Nacional Autónoma de México, Ciudad Universitaria, México D. F., Mexico*

[3] *Departamento de Matemáticas, Escuela Superior de Física y Matemáticas, Instituto Politécnico Nacional, México, D. F., Mexico*

The phenomenon of electrification is the accumulation of electric charge in a material. Polymers may become electrified when subjected to intense friction during their processing or under working conditions and the accumulated electric charge may change their adhesion and friction properties. In this work, a study of the influence of molecular weight and chain mobility on the electrification of linear low-density polyethylenes under continuous extrusion is presented. The use of different die materials, polymer processing additives, as well as slip and no slip flow conditions allowed the identification of two different mechanisms for electric charge generation in the melts; namely, the stripping of an electrical double layer acting in the absence of slip, and dynamic frictional electrification, or tribocharging acting under strong slip conditions. The magnitude of the electric charge was found to increase with polymer molecular weight and die length, and exhibited a local maximum as a function of the average velocity of the melt in both cases. The height of the maximum increased along with the molecular mobility. The experimental results were compared with the numerical solution of the equation of continuity for charge transport and it is shown that it does not describe the experimental results because it does not consider the additional mechanism of charge generation introduced by strong slip at the die wall. POLYM. ENG. SCI., 48:386–394, 2008. © 2007 Society of Plastics Engineers

INTRODUCTION

The phenomenon of electrification is the accumulation of electric charge in a material. The electric charge on a polymeric surface is usually removed by the air with the help of antistatic agents commonly added during its processing. Therefore, in the presence of a low density of charge in an insulator the electrification phenomenon is scarcely visible. Nevertheless, the electric charge accumulated in a polymer may be substantially increased when it is subjected to intense friction during processing or under working conditions. Such an electric charge build-up in a polymer may be annoying or represent potential explosive hazards [1]. In addition, it may produce sticking to equipment in post-processing operations [2], and it is not surprising that the presence of trapped charges at a polymeric surface affects its adhesion and friction properties [3].

The phenomenon of electrification in polymeric solids is well known and depends on the chemical nature of the surfaces into contact, as well as on the working conditions as temperature, sliding velocity and environment [4, 5]. The charge transfer in polymer-metal contacts is generally assumed to be due to electrons, but ion or material transfer might be also relevant.

The phenomenon of electrification has been scarcely studied in the case of polymer melts. The first systematic studies in this field where those by Vinogradov and coworkers [6, 7], who used measurements of electric charge on extrudates to evidence wall slip in the spurt flow regime during the capillary extrusion of flexible polymers, mainly rubbers. Also, by the same time Taylor et al. [8] measured the electrification of polystyrene, low-density polyethylene, and polycarbonate melts under stable capillary flow.

The electrification of polymer melts during extrusion was first attributed to a process of dynamic friction arising from a failure of the no slip boundary condition at the die wall [6]. Dreval et al. [7] showed that the accumulated

Correspondence to: Prof. José Pérez-González; e-mail: jpg@esfm.ipn.mx
Contract grant sponsor: SIP-IPN; contract grant number: 2005-0479.
DOI 10.1002/pen.20900
Published online in Wiley InterScience (www.interscience.wiley.com).

charge density varied with the die length, reaching eventually a maximum, and increased along with polymer molecular weight. Such a maximum was also observed as a function of the sliding velocity. Lastly, Dreval et al. [7] showed that the time–temperature superposition principle was applicable to their data, which evidenced the contribution of segmental mobility of the chains to electrification of the melt.

On the other hand, Taylor et al. [8] ascribed the electrification phenomenon during extrusion to the separation by flow of an electrical double layer formed at the interface between the polymer melt and the die wall. Also, Taylor and coworkers reported a maximum in the electric charge for polystyrene filled with Al_2O_3, which was attributed to an increase in electrical conductivity, as predicted by the continuity equation for electric charge transport in a tube (see the next section).

The electrification phenomenon in polymer melts did not receive further attention until recently, when Pérez-González and Denn [9] reported for the first time the electrification of linear low-density polyethylene (LLDPE) under continuous extrusion through a brass die. In agreement with the hypothesis by Vinogradov et al. [6] and Dreval et al. [7], the phenomenon was attributed to strong slip occurring at the die wall. In contrast, the electrification phenomenon was not observed for the same polymer when using a stainless steel die where slip was absent at even higher shear stress values. Thus, the electrification of the melt was suggested as a signature of slip at the die wall. This fact was later verified and used by Pérez-González [10] and Pérez-Trejo et al. [11] to study the slip and triboelectrification phenomena of LLDPE melts. In these last two works, there was a systematic coincidence of the simultaneous appearance or disappearance of both, strong slip conditions and electric charge on the extrudates. The same electrification phenomenon has been identified in a series of experiments with other linear polyethylenes through dies made up of copper alloys, as well as in the presence of fluropolymer polymer processing additives (FPPA). In all cases, electrification was accompanied by strong slip conditions [12–14], and Pérez-González [10] reported an empirical relationship between the slip velocity and the electric charge in the stable flow regime prior to the stick-slip. On the other hand, the magnitude of the electric charge was reported to increase with temperature [11].

Independent measurements of electric charge during the injection moulding of polypropylene [15], and during the capillary extrusion of LLDPE [16], have been recently reported. Tonon et al. [16] detected electrification in the sharkskin regime during the extrusion of LLDPE and suggested that both mechanisms, slip and a double layer effect, could be acting, even though they did not provide conclusive evidence of slip. These authors also found that the electric charge data followed an Arrhenius behavior, which according to Dreval et al. [7] makes a link with the molecular mobility of the polymer chains. In a more recent work [17], Flores et al. attributed the electrification observed in LLDPE extruded with processing aids to the effect of an electrical double layer.

Finally, Pérez-González [18] showed that there is indeed an electric charge in the sharkskin regime of LLDPE, but it is smaller in magnitude as compared with that measured under true slip flow for comparable shear rates. This result suggested a mechanism different from tribocharging in the sharkskin regime. Also in the same work, oscillation of the electric charge during the stick-slip indicated that there are flow conditions in which the generated electric charge is drastically decreased or may change its polarity, which is in agreement with the existence of more than one electrification mechanism during the extrusion of linear polyethylenes.

In the present work, we report a study of the influence of molecular weight on the electrification of metallocene catalyzed linear low-density polyethylene (mLLDPE) melts under continuous extrusion. The use of different die materials, as well as FPPA allowed the promotion of slip and no-slip flow conditions, from which two different mechanisms of charge generation were identified; the stripping of an electrical double layer one acting in the absence of slip and dynamic frictional electrification (tribocharging) acting under strong slip conditions. The magnitude of the electric charge was found to increase with polymer molecular weight and die length, and exhibited a local maximum as a function of the average fluid velocity. Finally, we solved the equation of continuity for charge transport and show that it does not describe the experimental results because it does not consider the additional mechanism of charge generation introduced by strong slip at the die wall.

THEORETICAL CONSIDERATIONS

The charging process at a solid/liquid interface is assumed to arise from the presence of an electrical double layer, which in commercial polymers may appear by the presence of additives and impurities. The electric charge density $q(r,z)$ in a liquid flowing through a capillary is dependent on its radial (r) and axial (z) positions (Fig. 1), and satisfies the general equation of continuity [19]:

$$v_z(r)\frac{\partial q(r,z)}{\partial z} - \frac{D_c}{r}\left(r\frac{\partial q(r,z)}{\partial r}\right) + \frac{q(r,z)}{\tau} = 0 \qquad (1)$$

where $v_z(r)$ is the fluid velocity profile for a fully developed flow, D_c is the diffusion coefficient of the charged species and $t = \varepsilon\rho$ is the dielectric relaxation time of the liquid given by the product of its permittivity (ε) and resistivity (ρ), respectively. *Equation 1* includes the contributions of diffusion, conduction, and convection to the total electric charge density in the fluid. Then, *Eq. 1* needs to be solved with proper boundary conditions in order to determine the charge distribution across the capillary (see Fig. 1). Analytic solutions of *Eq. 1* are limited to cases where the velocity is independent of the radial and axial positions. Gavis and Kosman [19] obtained a solution for a flat velocity

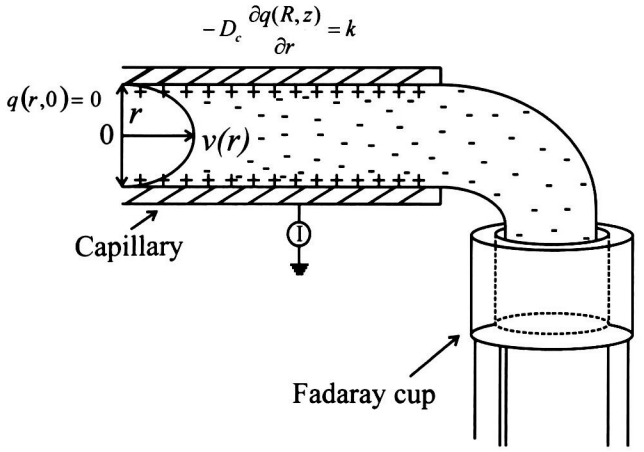

FIG. 1. Schematic representation of the electrification process and boundary conditions.

profile, and Taylor et al. [8] for a Newtonian parabolic one in limiting cases. However, in the more general case of a non-Newtonian velocity profile, *Eq. 1* has to be solved numerically. Once *Eq. 1* is solved for $q(r,z)$, a charge rate or streaming current (i) may be calculated by [8]:

$$i = 2\pi \int_0^R rq(r,L)v_z(r)dr \qquad (2)$$

In which, R and L are the radius and length of the capillary, respectively. Usually, it is the electric charge rate or streaming current given in *Eq. 2* what is measured during the experiments. Ideally, $q(r,z)$ obtained from the solution of *Eq. 1* and put into *Eq. 2* should be the same as the streaming current determined by experiments.

EXPERIMENTAL PROCEDURE

The polymers used in this work were a family of mLLDPE produced by Aldrich. These are copolymers of ethylene and butene whose main characteristics are reported in Table 1. The polymers were provided in pellets and reported with antioxidants, only. Unfortunately, the same type of polymers with the same melting point was not available. The variations in the melting points are likely due to differences in the comonomer contents.

The molecular mass distributions (MMD) of the polymers were calculated from oscillatory shear experiments in a MCR 301 Physica rheometer and the associated software Rheoplus™ 2.81. The oscillatory experiments were carried out in the linear viscoelastic regime at different temperatures to construct a master curve, from which, the continuous relaxation time spectrum was calculated. From this, the MMD for each polymer was obtained by using the Doi's kernel, which consists of a sum of single exponential relaxation terms. The obtained MMDs for the different polymers are consistent with those reported by other authors using gel permeation chromatography for similar melt indexes mLLDPEs [20].

TABLE 1. Characteristics of the polymers used

Polymer	MFI (g/10 min)	T_m (°C)	M_w (g/mol)	M_n (g/mol)	Density (g/cm^3)
A	0.8	60	93,200	49,930	0.880
B	1.2	92	89,670	45,450	0.900
C	3.0	60	69,430	37,200	0.878
D	4.5	98	62,510	25,370	0.905

Flow experiments were performed at a temperature of 200°C in the die with a computer operated Brabender single screw extruder of 0.019 m in diameter and a length to diameter ratio of 25/1. The temperature profile for the four different heating zones of the extruder was as follows, 160, 180, 200, and 200°C, respectively. Because of the low melting point of the polymers, a constant air flow was provided in the feeding section of the extruder in order to avoid melting of the polymers in such region.

The pressure drop between capillary ends was measured with a Dynisco™ pressure transducer. Two capillaries made up of 464 naval brass and stainless steel, respectively, both with $L/D = 20$ and $D = 0.001$ m were used. Slip and no slip flow conditions were investigated. A fluropolymer polymer processing additive (FPPA, FX-9613 from 3M) was used in order to promote slip. Since the magnitude of slip depends on the cleanness of the die internal surface, the extruder and dies were first cleaned with a purging compound (Unipurge™ from Union Carbide). Then, either the pure polymers or their blends with 0.1 wt% of FPPA was allowed to flow in the system for more than 1 h before starting the measurements, in order to remove residuals of the purging compound. Slip flow was recognized by the disappearance of sharkskin distortions, by a decrease in the pressure drop at constant screw velocity and by the presence of electric charge on the extrudates.

The procedure for the electrical measurements was similar to the one used and described in detail by Pérez-González [18], this is sketched in Fig. 2. The only difference in the present work was the use of a Faraday cup instead of the probe to detect the charges on the extrudates. In contrast to measurements by using a probe, the use of the Faraday cup

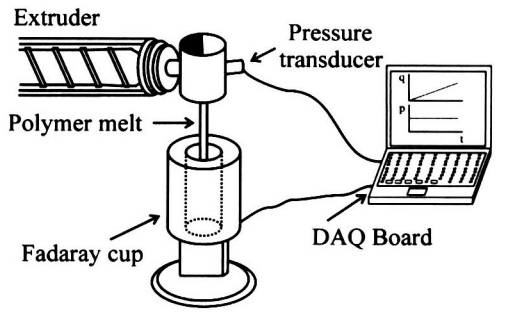

FIG. 2. Schematic representation of the experimental set-up.

DOI 10.1002/pen

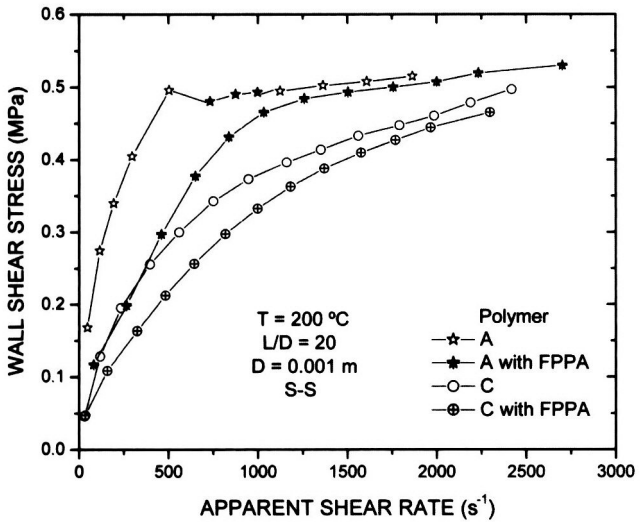

FIG. 3. Flow curves obtained for the polymers A and C with and without FPPA using a stainless steel die (S-S). Dark symbols represent the average shear stress values in the stick-slip regime.

permits the determination of the absolute density of charge on the extrudates. The charge acquired by the Faraday cup and the pressure drop were monitored simultaneously via a data acquisition board coupled to a computer. In most cases, the charge and pressure drop data presented in this work were acquired at a rate of 10 points/s, but this rate was changed to 100 points/s to study the unstable stick-slip flow regimes.

RESULTS AND DISCUSSION

Flow Curves and Slip

The standard formulas to evaluate the capillary flow behavior of non-Newtonian liquids are $\tau_w = D\Delta p/4L$ for the wall shear stress, and $\dot{\gamma}_{app} = 32Q/\pi D^3$ for the apparent shear rate. In these formulas, D and L are the diameter and length of the capillary, respectively, Δp is the pressure drop between capillary ends and Q_{exp} is the experimentally measured volumetric flow rate. To obtain the true shear rate for a non-Newtonian fluid the Rabinowitsch correction must be performed, but this is not relevant for the purposes of this work, since the whole analysis of the electrification of the melts is performed in terms of the average and slip velocities. The flow curves obtained using the stainless steel die and different molecular weight (M_w) polymers are shown in Figs. 3 and 4. The plots have been arranged to compare polymers with different M_w but similar melting points (polymers A and C, and polymers B and D, respectively). This allows for the comparison of the flow behavior at similar conditions of chain mobility. Data obtained when using the FPPA are also included in both figures.

Several aspects of the flow curves may be distinguished in Figs. 3 and 4. First, it is evident that the polymer viscosity increases with increasing M_w. Also, polymers A and B, Figs. 3 and 4, respectively, show a stick-slip behavior that is not present for the smaller M_w ones, C and D. It is likely that the critical level of entanglements is not reached in the two smaller molecular weight polymers, which prevents the stick-slip to occur [21]. Then, there is a clear difference between the flow curves for the pure polymers and with FPPA, since the shear stresses are higher for the pure polymers at a given apparent shear rate; this is an evidence of slip when using the FPPA. In addition, it can be observed that the presence of strong slip helps to eliminate the stick-slip instabilities for polymers A and B, and produces monotonic flow curves for all the polymers in the shear stress range studied.

A slightly different behavior is observed when extrusion is performed through the brass die; the results obtained with polymer A are shown in Fig. 5. In this case, pressure drops are decreased for the pure polymer as compared to the observed when using the stainless steel die (see Fig. 3). In addition, the stable region extends to higher shear rate values and the stick-slip appears at higher shear stresses than in the case of the stainless steel die. Such an increase of the critical shear stress for this polymer has been attributed to enhanced adhesion of the macromolecules at the brass die wall once the effect of slip disappears [18]. In the presence of the FPPA, however, the behavior is similar to that observed for the polymer with FPPA in the stainless steel die, namely, flow curves of the polymer with FPPA in the brass die are monotonic again and exhibit smaller pressures as compared with the pure polymer, which is also consistent with the presence of slip during the experiments. This result is consistent with a previous report by Pérez-Trejo et al. [11] in which they compared the electrification when using pure LLDPE as well as with FPPA through a brass die. Below, only the results obtained with the stainless steel die will be discussed.

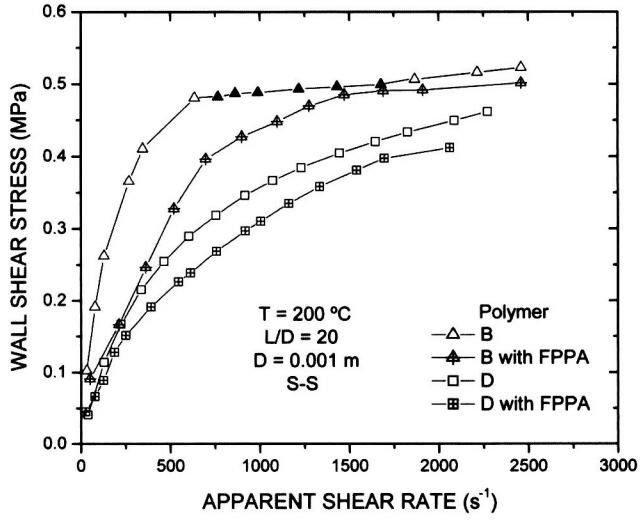

FIG. 4. Flow curves obtained for the polymers B and D with and without FPPA using a stainless steel die (S-S). Dark symbols represent the average shear stress values in the stick-slip regime.

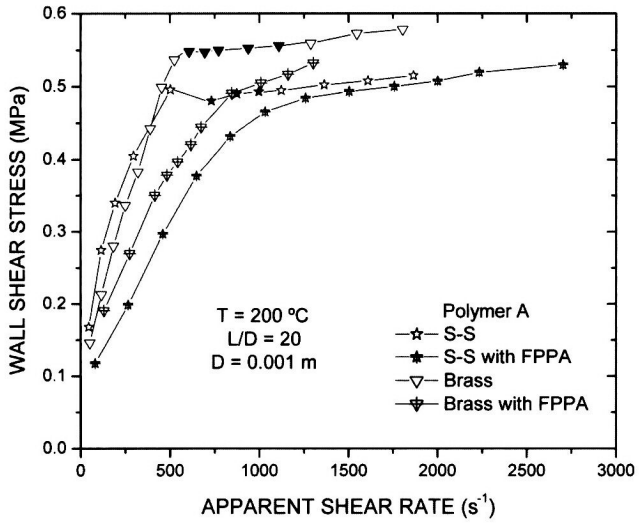

FIG. 5. Flow curves obtained for the polymer A with and without FPPA using a stainless steel (S-S) and a brass die. Dark symbols represent the average shear stress values in the stick-slip regime.

A slip velocity (v_s) can be calculated for the regions of stable flow for the mLLDPE + FPPA systems in the stainless steel die by using the equation [22]:

$$v_s = \frac{4(Q_s - Q_{f\text{-}s})}{\pi D^2} \tag{3}$$

where Q_s and $Q_{f\text{-}s}$ represent the volumetric flow rates with slip and free of slip, respectively, for a given shear stress. In the case of polymers A and B only the stable data before the stick-slip were considered to calculate the slip velocity. From the data in this work, the slip velocity was found to increase with the shear stress and the M_w value of the polymer (see also Fig. 6), in agreement with previous reports [22].

The ratio between the slip and average fluid velocities is shown in Fig. 6 for all the polymers. As previously reported by Pérez-González and de Vargas [22] and Pérez-Trejo et al. [11], there is a maximum in the contribution of the slip velocity to the total average fluid velocity, which has been attributed to the influence of shear thinning in the melt. For polymer A the maximum probably appeared at shear stresses below the studied range, which was limited by the lowest available velocity in the extruder.

Electrical Measurements

Evidence of Two Different Mechanisms for Charge Generation. The electric charge build-up was measured for all the polymers under the different extrusion conditions. The evolution of the charge accumulation or streaming current is directly related to the flow conditions. Under steady flow the streaming current was constant, but there was an oscillating behavior in the stick-slip regimes, as expected from the unstable flow conditions [18].

On the other hand, the data obtained from the electrical measurements performed on the pure polymers as well as with FPPA are shown separately in Fig. 7a and b for comparable melting points polymers. The charge density (charge per unit volume) calculated from the measured streaming current is plotted as a function of the average fluid velocity in each case. Results in Fig. 7a and b are particularly interesting, since for all the polymers, the electric charge measured under strong slip conditions is almost one order of magnitude higher than that measured without slip at comparable velocities. Furthermore, with exception of polymer D, there is an inversion in the sign of the electric charge between the pure polymer and with FPPA for the other three, which in agreement with Pérez-González [18] is indicative of a change at the melt die interface. The same behavior was observed for the pure polymer through the brass die, i.e., without the influence of FPPA [see also 10, 11, 18], which suggests that two different electrification mechanisms act under slip and no slip flow, respectively.

The existence of two different mechanisms of charge generation is further supported by the electrification data of polymer A through dies made up of stainless steel and brass, respectively, such data are presented in Fig. 8. It is evident from this figure that in the presence of slip (when using the brass die with and without FPPA, and when using the stainless steel die with FPPA) the electric charge is significantly increased as compared with the case without slip (the case when using the pure polymer through the stainless steel die). Note that the electric charge under slip can not be only attributed to an electrical double layer caused by the FPPA, as has been recently done [17], since the same order of magnitude of the electric charge is measured when using the brass die without FPPA.

Figure 9a and b show the radial charge distributions obtained from the solution of *Eq. 1* under no slip and slip

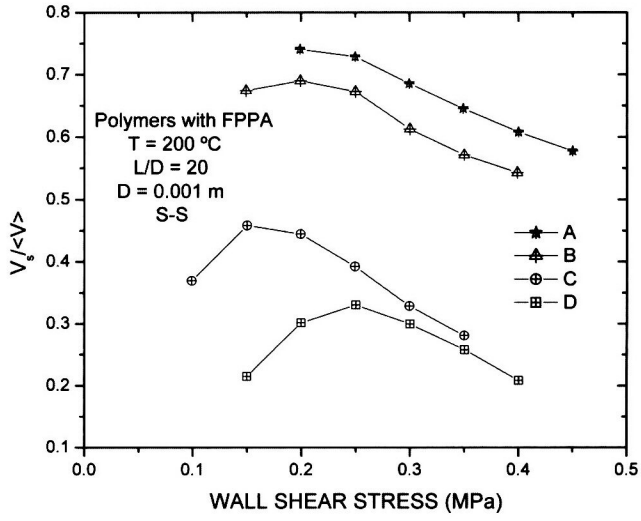

FIG. 6. Plots of the ratio between the slip velocity and the average velocity in the stainless steel die as a function of the wall shear stress for the different polymers with FPPA.

DOI 10.1002/pen

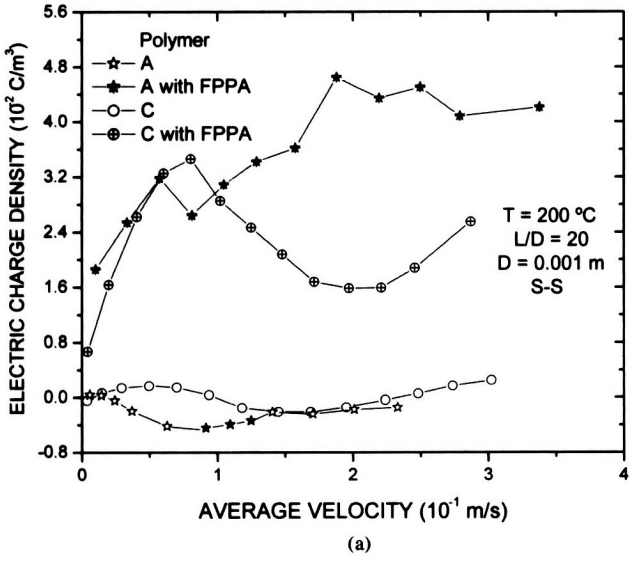

FIG. 7. Plots of the electric charge density measured as a function of the average melt velocity with and without FPPA using a stainless steel die (S-S) for the polymers, (a) A and C, (b) B and D. Dark symbols represent the average values in the stick-slip regime.

flow conditions, respectively, for polymer C at different axial positions through a capillary of $L/D = 20$. Electrical data from Taylor and Lewis [23] for a polyethylene at $T = 165°C$ were used in solving *Eq. 1*, along with the boundary conditions stated in Fig. 1 and considering the power-law velocity profile $v_z(r)$ given by:

$$v_z(r) = v_s + \left(\frac{\tau_w}{m}\right)^{\frac{1}{n}} \frac{nR}{n+1}\left[1 - \left(\frac{r}{R}\right)^{\frac{n+1}{n}}\right] \qquad (4)$$

where v_s is the slip velocity at the chosen wall shear stress (t_w), R is the capillary radius, and "$n = 0.58$" and "$m = 0.005$ MPa.s^n" are the power law parameters. The main trends of the electric charge density for a given value of the fluid velocity are easily observed in Fig. 9a and b; it increases and its influence extends towards the capillary axis as the fluid moves along the capillary (Fig. 9a). The fact that the electric charge density changes along the tube for a given velocity means that there is a development of the double layer, and that a certain tube length is necessary to have a fully developed charge profile. On the other hand, an increase in the fluid velocity tends to decrease the extent of the double layer because diffusion of charges is restricted by fluid convection, then, the larger the fluid velocity the narrower the double layer (compare the results in Fig. 9a and b).

On the other hand, the streaming current was calculated from the integral (2) using the electric charge density obtained from the solution of *Eq. 1* with and without slip. The corresponding values are plotted in Fig. 10a, as well as in Fig. 10b along with the experimental values for polymer C. It can be seen from Fig. 10a that the calculated streaming current is an increasing function of the average velocity, and as expected, it increases in the presence of slip. Also, it can be observed from Fig. 10b that the calculated streaming current is comparable with that measured in the experiments without slip, but is very small in magnitude as compared with that observed under strong slip.

Because of the presence of any impurities in the polymers, the electric charge generation arising from the stripping of a double layer is very likely, in agreement with Taylor et al. [8], and may be responsible for the charge build-up in the absence of slip. However, the double electric layer mechanism can not account neither for the increase of almost one order of magnitude in the electric charge nor for the sign reversing occurring in the presence of slip. As shown in Fig. 10b, the only consideration of a nonzero velocity at the die wall in the solution of *Eq. 1* is not enough to reproduce the observed experimental results in the pres-

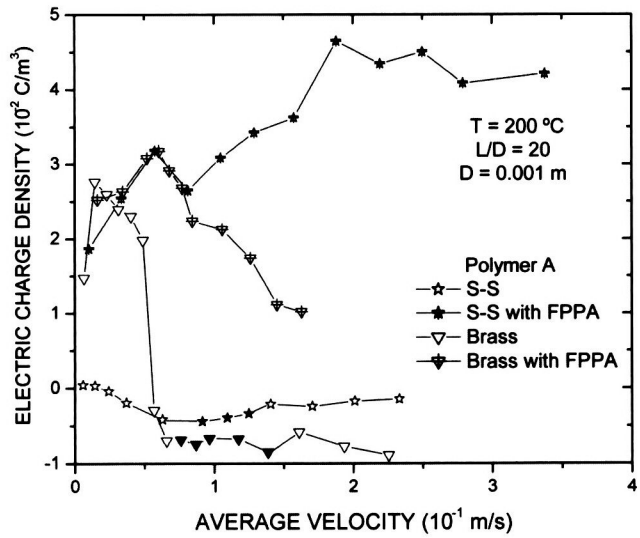

FIG. 8. Plots of the electric charge density as a function of the average melt velocity for polymer A with and without FPPA using a stainless steel (S-S) and a brass die. Dark symbols represent the average values in the stick-slip regime.

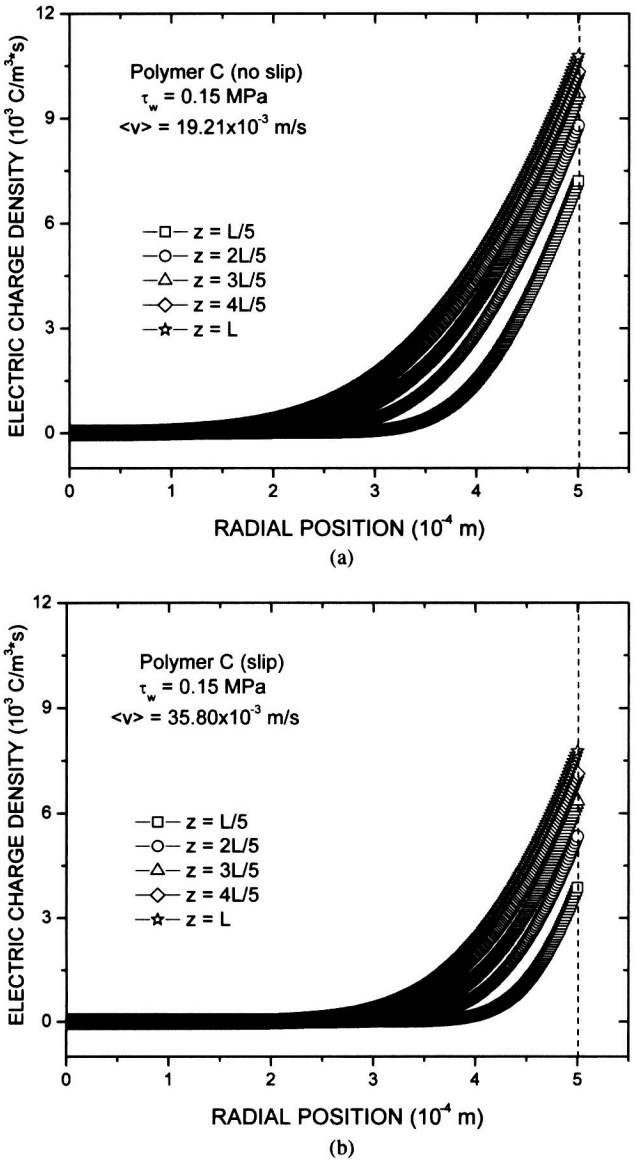

FIG. 9. Plots of the calculated electric charge density as a function of the "r" coordinate for different axial positions for polymer C, (a) without slip, (b) with slip.

ence of slip. In the present experiments, the dynamic friction at the melt/die wall interface may be increasing the electrical charge by the observed order of magnitude and modifying the charge transfer at the die wall.

In the case of extrusion with strong slip, it is not possible to separate the contribution of a double layer from the tribocharging in the total density of charge. However, the presence of a large density of charge and the reversing of its sign may be considered as indicative of the existence of a tribocharging mechanism or slip at the die wall. Even though several researchers had already suggested the possible existence of both mechanisms for the electrification of polymer melts, as far as we know, this is the first report giving clear evidence of their existence for a given polymer and their link to the flow conditions, namely, slip or not slip flow.

Another important issue to highlight from results in Figs. 7a and b and 8, is the fact that the charge density has a local maximum for the experiments with slip. This does not occur for the experiments without slip at similar average velocities, in which the electric charge seems to be an increasing or decreasing function of the average velocity in the studied range. In fact, the curves of electric charge density versus average velocity in the presence of slip are complex and describe several regimes. Thus, not only a local maximum, but also a local minimum appears for some M_w values. Moreover, the electric charge build-up increases to still higher values as the average velocity goes close to the melt fracture regime.

The existence of a maximum in the electric charge of LLDPE was reported by Pérez-Trejo et al. [11] for different temperatures. These authors attributed the existence of the

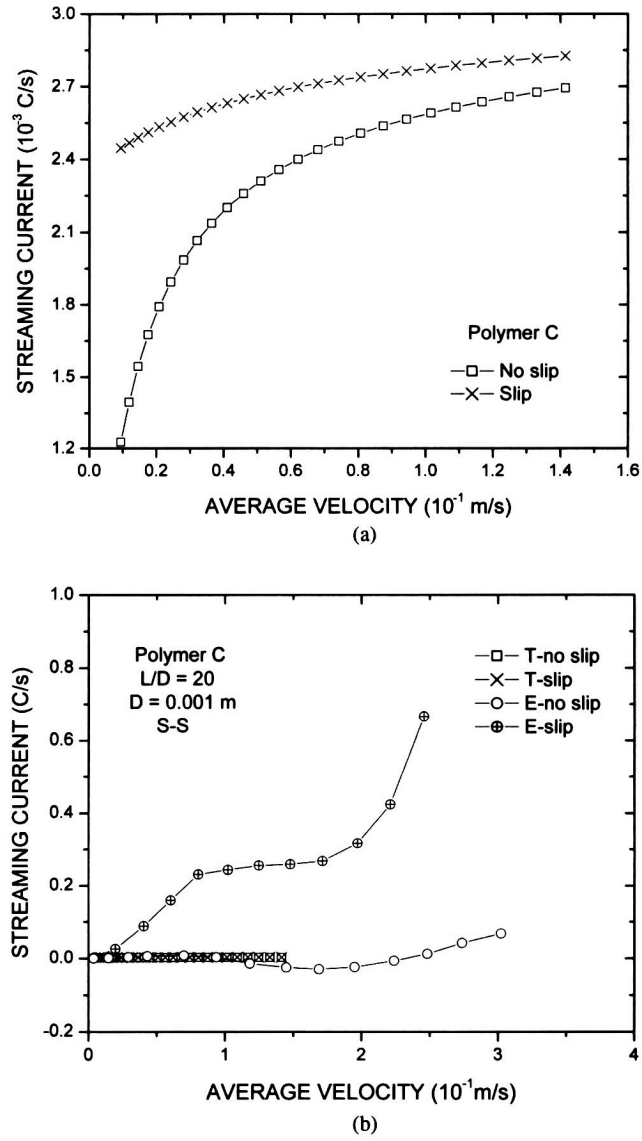

FIG. 10. Plots of the streaming current as a function of the average velocity with and without slip for polymer C. (a) Calculated data (T); (b) Comparison of calculated (T) and experimental data (E).

DOI 10.1002/pen

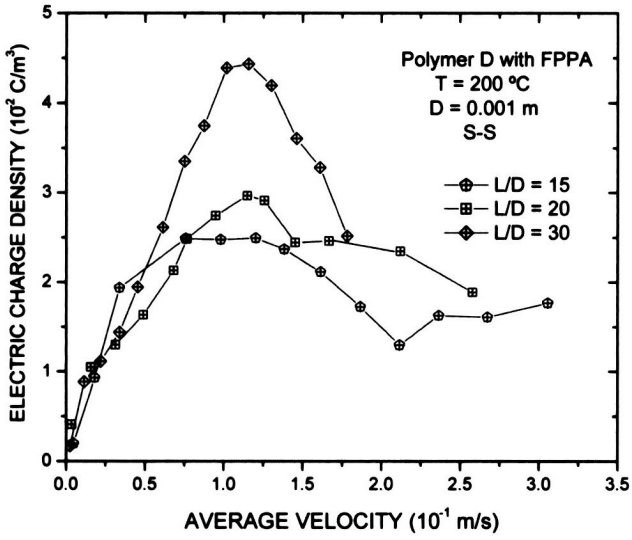

FIG. 11. Plots of the electric charge density as a function of the average melt velocity with FPPA using stainless steel dies (S-S) of different *L/D* ratios for polymer D.

maximum to a decrease in the contribution of the slip velocity to the whole average velocity because of a coincidence of the critical shear stress for both maxima. Such a behavior was related with shear thinning in the melt. In the present work, however, the critical shear stress for the maximum in the contribution of slip to the average fluid velocity for the different polymers (Fig. 6) does not agree with that corresponding to the maximum charge (Figs. 7a and b and 8). Then, another variable related to the molecular properties of the melts might be involved in the process of electrification.

Influence of M_w *on Melt Electrification*

It can be observed from Fig. 7a and b that at low velocities the magnitude of the electric charge is higher for the polymers with the higher M_w values. Since the polymers studied have a similar polydispersity, then the main differences in their electrification behavior are due to the differences in molecular weight. Thus, the maximum in the electric charge density appears at lower average velocities and has a smaller magnitude for the polymers with higher M_w values than for the lower ones and similar melting point. This behavior is in agreement with that reported by Dreval et al. [7] in the sense that the magnitude of the electric charge first increases with M_w, but the maximum is higher as the chains mobility is increased or the M_w is decreased. In other words, the mobility of the polymer chains play an important role in the process of electrification.

Ohara [24] suggested that the magnitude of the electric charge was dependent on the number of contacts at the polymer/metal interface. In the presence of slip of course, it is expected that not only the contact points are important for the electrification process, but also the number of sliding contacts. In fact, Pérez-González [18] suggested that a higher number of adsorbed chains or nonsliding contacts at the die wall tend to decrease the magnitude of the electric charge. In this view, the different regimes observed in the electric charge versus stress curves might be related to different slip flow regimes. This is an issue that needs to be further explored.

Dependence of the Electrification Phenomenon on the Capillary L/D Ratio

Figure 11 shows measurements of the electric charge density as a function of the average velocity for polymer D with FPPA in capillaries of different *L/D* ratio and same diameter. It can be seen from this figure that the trend of the electric charge density is to increase along with the capillary length, and that the longer the capillary the higher the maximum, whose critical shear stress seems to be independent of the *L/D* ratio. This increase in the electric charge build-up when increasing the die length is consistent with predictions of the theory of the electrical double layer (see Fig. 9a and b). However, as previously discussed, the existence of a local maximum and the differences in the values of the electric charge density between slip and no slip flow for fixed conditions of temperature and polymer conductivity can not be explained on the basis of a stripping of a double layer. This set of results evidence once again that there are two different mechanisms for the electric charge generation, namely, the stripping of an electrical double layer and tribocharging, which act under no slip and slip conditions, respectively. The fact that the magnitude of the electric charge density increases with the die length may be explained on the basis of an increase in the number of sliding contacts. It must be pointed out, however, that for longer dies than those used in this work the influence of pressure on polymer viscoelasticity and slip may lead to a decrease in the number of the sliding contacts, and therefore, in the electrification of the melt.

Finally, it is important to point out that the results in this work are just at the beginning of the explorations in the area of electrification of polymer melts. A complete description of the phenomenon requires the identification of the basic mechanisms (which has been done in this work), and then their proper inclusion, very likely via boundary conditions, on a mathematical model. Also, it must be pointed up that slip at the die wall produces electrification of the melt, but electrification of the melt does not imply the presence of slip; the identification of the mechanism for charge generation may be done via the magnitude of the electric charge as well as by changes in its polarity.

CONCLUSIONS

From the results presented in this work it can be concluded that there are two different mechanisms for electric charge generation in polymer melts, namely, the stripping of an electrical double layer acting in the absence of slip, and dynamic frictional electrification or tribocharging act-

ing under strong slip conditions. Even though slip at the die wall produces electrification of the melt, the last does not implies the presence of slip; the identification of the mechanism for charge generation may be done via the magnitude of the electric charge density as well as by changes in its polarity. On the other hand, the magnitude of the electric charge density increases with the polymer molecular weight and die length, and exhibited a local maximum as a function of the average velocity in the presence of slip. Meanwhile, the height of the maximum increases along with the molecular mobility. Finally, the experimental results do not agree with the numerical solution of the equation of continuity for charge transport, because it does not consider the additional mechanism of charge generation introduced by strong slip at the die wall. Further work is still necessary to fully understand and describe the phenomenon of electrification in polymer melts.

ACKNOWLEDGMENTS

F. R-G had a CONACYT and DGEP-UNAM scholarships. J. P-G, L.deV, E. M and J. G. G-S are COFFA-EDI-EDD fellows.

REFERENCES

1. D.M. Taylor and P.E. Secker, *Industrial Electrostatics: Fundamentals and Measurements*, Research Studies Press LTD., England, 67–128, (1994).
2. T. Guadarrama-Medina, J. Pérez-González, and L. de Vargas, *Rheol. Acta.*, **44**, 278 (2005).
3. C. Guerret-Piecourt, S. Bec, and D. Treheux, C. R. Acad. Sci. Paris, t. 2, Série IV, 1 (2001).
4. J. Lowell and A.C. Rose-Innes, *Adv. Phys.*, **29**, 947 (1980).
5. C.C. Ku and R. Liepins, *Electrical Properties of Polymers*, Hanser, Germany, 223 (1987).
6. G.V. Vinogradov, A.Y. Malkin, Y.G. Yanovskii, E.K. Borisenkova, B.V. Yarlykov, and G.V. Berezhnaya, *J. Polym. Sci. Part A-2: Polym, Phys.*, **10**, 1061 (1972).
7. V.Y. Dreval, G.V. Vinogradov, and V.P. Protasov, in *Proc. IX Intern. Congress on Rheology, Vol. 3*, B. Mena, A. García-Rejón, and C. Rangel-Nafaile, Eds., México, 185 (1984).
8. D.M. Taylor, T.J. Lewis, and T.P.T. Williams, *J. Phys. D: Appl. Phys.*, **7**, 1756 (1974).
9. J. Pérez-González and M.M. Denn, *Ind. Eng. Chem. Res.*, **40**, 4309 (2001).
10. J. Pérez-González, *J. Rheol.*, **45**, 845 (2001).
11. L. Pérez-Trejo, J. Pérez-González, L. de Vargas, and E. Moreno, *Wear*, **257**, 329 (2004).
12. V. Garrido Cruz, BS Thesis, Intituto Politécnico Nacional, México (2001).
13. R. Flores Suárez, BS Thesis, Instituto Politécnico Nacional, México (2003).
14. L. Pérez-Trejo, J. Pérez-González, L. de Vargas, and E. Moreno, in *Proc. VI Eur. Conf. Rheol.*, H. Münstedt, J. Kaschta, and E. Merten, Eds., Germany, 159 (2002).
15. M. Murtomaa, S. Kankaanpää, J. Nurmio, M. Leino, J. Mäkelä, P. Järvelä, E. Laine, and V.P. Lehto, *Inst. Phys. Conf. Ser.*, **178**, 83 (2004).
16. S. Tonon, A. Lavernhe, F. Flores, A. Allal, and C. Guerret-Piécourt, *J. Non-Newtonian Fluid Mech.*, **126**, 63 (2005).
17. F. Flores, D. Burlot, A. Allal, and C. Guerret-Piecourt, *J. Non-Newtonian Fluid Mech.*, **134**, 8 (2006).
18. J. Pérez-González, *J. Rheol.*, **49**, 1 (2005).
19. J. Gavis and I. Koszman, *J. Colloid Sci.*, **16**, 375 (1961).
20. K.C. Seavey, Y.A. Liu, N.P. Khare, T. Bremmer, C.-C. Chen, *Ind. Eng. Chem. Res.*, **42**, 5354 (2003).
21. S.Q. Wang, *Adv. Polym. Sci.*, **138**, 227 (1999).
22. J. Pérez-González and L. de Vargas, *Polym. Eng. Sci.*, **42**, 1231 (2002).
23. D.M. Taylor and T.J. Lewis, in *4th Int. Conf. Conduction and Breakdown Dielectric Liquids*, T.J. Gallagher, Ed., Ireland, 176 (1972).
24. K. Ohara, *Inst. Phys. Conf. Ser.*, **48**, 257 (1979).

DOI 10.1002/pen